



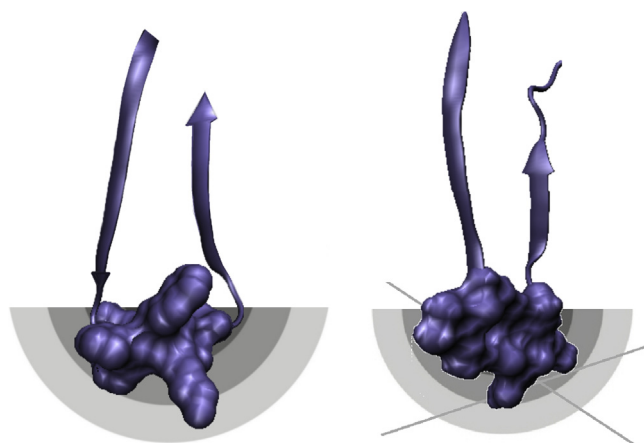
# Specificity of amino acid sequence and its role in secondary and supersecondary structure generation

Mateusz Banach<sup>1</sup>, Irena Roterman<sup>1</sup>

<sup>1</sup>Department of Bioinformatics and Telemedicine, Jagiellonian University—Medical College, Krakow, Poland

## Contents

Short fragments of polypeptide playing the role of linkers between $\beta$ -strands belonging to $\beta$ -sheets	208
Short peptides	211
Alternative structures solve the problem of minimization of the hydrophobic area on the surface generating the ribbon-like structural forms	212
References	214



*Schematic presentation of loops (7 aa) linking two  $\beta$ -strands (fragments of  $\beta$ -sheets). The left one — helical form represents fuzzy oil drop distribution of*

*hydrophobicity. The right one not able to generate the helical form represents the status recognized as amyloid seed in amyloids discussed in this work.*

The role of amino acids sequence — in particular 7aa fragment linking  $\beta$ -strands belonging to  $\beta$ -sheets can be easily visualized discussing examples of proteins generating the amyloid-like structures with the one representing the status accordant with the fuzzy oil drop model.



### **Short fragments of polypeptide playing the role of linkers between $\beta$ -strands belonging to $\beta$ -sheets**

Three polypeptides: A $\beta$ (15–40) — amyloid form (PDB ID: 2MPZ, “Iowa” mutant D23N) [1], chain C A $\beta$ (16–40) “packaged” with a synthetic protein in the complex with protein (PDB ID: 2OTK) [2] and C domain of light chain of IgG (PDB ID: 7FAB) [3] are taken as examples for the following analysis. These three structures contain  $\beta$ -strands belonging to  $\beta$ -sheets. These  $\beta$ -strands are linked by 7 aa fragment. The difference between selected proteins is their status as whole.

The C domain of light chain of IgG represents the hydrophobicity distribution accordant with fuzzy oil drop model. The status of 7 aa polypeptide chain fragments linking  $\beta$ -strands participating in  $\beta$ -sheet is examined. The fragments 22–28 of amyloid polypeptide chains (as observed in 2MPZ and 2OTK) and fragment 118–124 are compared to visualize the role and specificity of the sequence.

A proposed experiment involves modifying the 22–28 sequence to match the 118–124 fragment in the light chain of IgG. The amphipathic properties of the helical linker would likely mediate entropically advantageous contact with the aqueous solvent and therefore affect the structure as a whole. The 118–124 fragment is clearly predisposed toward a helical conformation, as listed in the database of chameleon sequences [4] where values greater than 1 indicate structural affinity, and the helical form scores more than 3 [4]. The amphipathic helix may be regarded as an alternative to a single dominant maximum which introduces strong discordance between O and T.

It is also interesting to note the status of the C-terminal fragment, which remains highly accordant in the immunoglobulin but is excessively hydrophobic in the A $\beta$  chain, despite remaining in contact with water (note the low values of O).

The  $\beta$ -hairpin is a common structural motif, found in many proteins. The  $\beta$ -hairpin discussed here differs in respect to proper  $\beta$ -hairpin

**Table 10.C.1** Fuzzy oil drop parameters for 7FAB, 2OTK and 2MPZ, along with fragments linking  $\beta$ -hairpin folds, compared to the corresponding linkers in the A $\beta$ (1–42) amyloid. Values listed in boldface represent linkers between separate  $\beta$  strands.

Structure	Fragment	RD		Correlation coefficient		
		T-O-R	T-O-H	HvT	TvO	HvO
7FAB (chain L)	104–204	0.320	0.237	0.588	0.809	0.825
	110–136	0.232	0.308	0.670	0.893	0.863
	<b>118–124</b>	<b>0.374</b>	<b>0.313</b>	<b>0.076</b>	<b>0.619</b>	<b>0.826</b>
	167–194	0.291	0.266	0.606	0.790	0.809
	<b>178–184</b>	<b>0.361</b>	<b>0.240</b>	<b>0.830</b>	<b>0.617</b>	<b>0.784</b>
2OTK (chain C)	16–40	0.592	0.290	0.279	0.494	0.603
	<b>22–28</b>	<b>0.613</b>	<b>0.356</b>	<b>–0.306</b>	<b>–0.018</b>	<b>0.866</b>
2MPZ (chain S)	15–40	0.627	0.467	0.355	0.351	0.616
	<b>22–28</b>	<b>0.637</b>	<b>0.503</b>	<b>–0.337</b>	<b>–0.320</b>	<b>0.938</b>

containing 7 instead of 4 residues building the turn. Thus, our analysis of the specificity of the 22–28 fragment is based on comparing it with an accordant  $\beta$ -hairpin (i.e. a structure consistent with the theoretical distribution of hydrophobicity). Table 10.C.1 provides a comparative overview of all presented structural motifs, including the  $\beta$ -hairpin fragment of A $\beta$ (16–40) in complex with two other chains which serve as permanent chaperones (PDB ID: 2OTK).

All presented fragments are of equal length (7 aa). Taken as a whole, the C domain of the IgG light chain follows a micelle-like distribution, with the linker exhibiting low RD and balanced values of FOD correlation coefficients. Radically different conditions are observed in the A $\beta$ (15–42) chain, for reasons illustrated in Fig. 10.C.1.

The observed differences seem to be caused by the fact that in the case of IgG the beta folds are linked by a helical fragment, which is largely accordant with the theoretical distribution (as evidenced by its low RD) thanks to its amphipatic character (see Fig. 10.C.1 and Table 10.C.1). In all presented cases, this linker (with a length of 7 aa) connects two separate  $\beta$  folds which belong to different  $\beta$  sheets. This is particularly evident in the case of A $\beta$ (15–40) (Fig. 10.C.2). Similarly, in the C domain of the IgG light chain the aforementioned helix (178–182) links two distinct  $\beta$  sheets. The intrinsic hydrophobicity which is able to generate the amphipatic helix

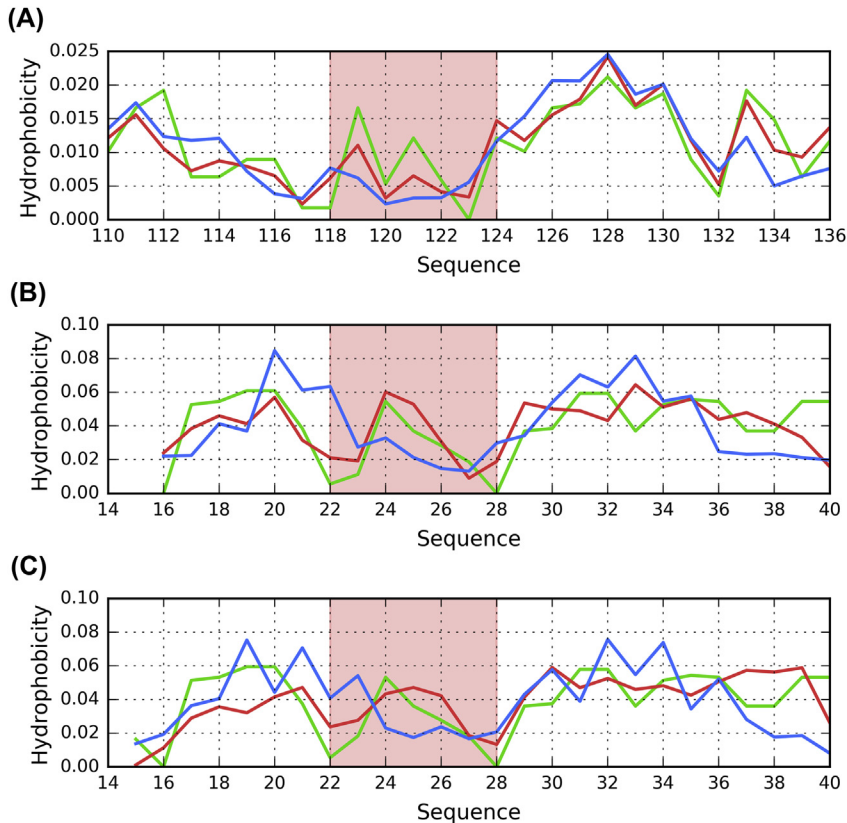


**Fig. 10.C.1** Theoretical (T, blue), observed (O, red) and intrinsic (H, green) hydrophobicity distribution profiles for selected structures containing the  $\beta$ -hairpin motif. (A) C domain of IgG light chain – fragment 104–204 of chain L of 7FAB (view limited to residues 110–136). (B) A $\beta$ (16–40) (chain C of 20TK). (C) A $\beta$ (15–40) (chain S of 2MPZ). The discussed  $\beta$ -hairpin folds present in the structures are marked by the red background.

(zigzag pattern) is present in immunoglobulin domain. This is not the case in A $\beta$ (15–40).

The visual analysis is possible due to the presentation of 3D structures of amyloid forms (Fig. 10.C.3). Two examples are shown in forms of  $\beta$ -strands linked by accordant helices (Fig. 10.C.4).

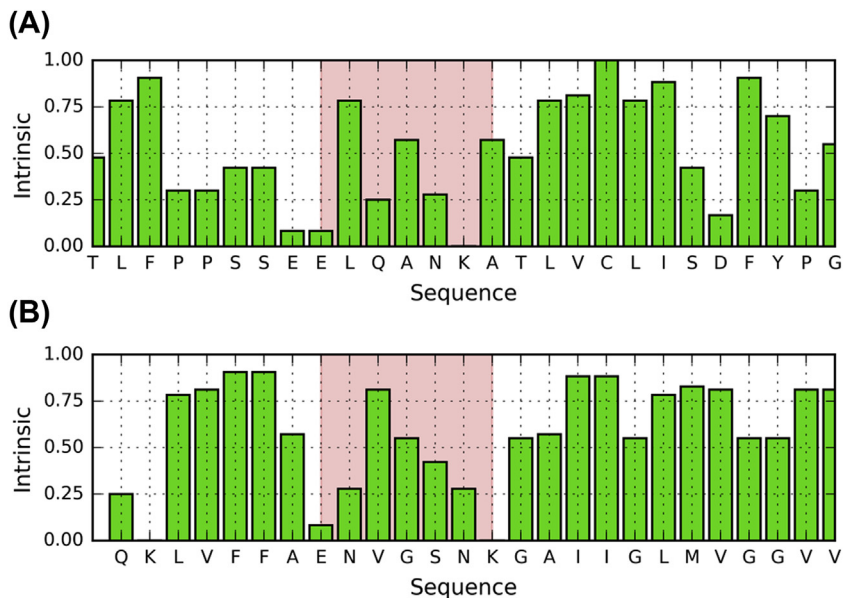


**Fig. 10.C.2** Intrinsic hydrophobicity distribution profiles for selected structures containing the  $\beta$ -hairpin motif. (A) C domain of IgG light chain — fragment 104–204 of chain L of 7FAB (view limited to residues 110–136). (B)  $A\beta(15-40)$  (chain S of 2MPZ). The discussed turns in  $\beta$ -hairpin folds present in the structures are marked by the red background. A zigzag form of intrinsic hydrophobicity for helical fragment be seen. This form produces the amphipathic helices.

## Short peptides

Experimental studies of short peptide sequences provide support for the hypotheses presented in this work. Sample sequences are described in Refs. [5,6].

It appears that the presented sequence fulfills the conditions for linear propagation criteria. Short peptides typically do not have a tertiary conformation and therefore cannot produce a spherical micelle. Thus, for structures such as the one shown in Fig. 10.C.5, a ribbonlike micelle remains the only option.

The specifics of protein-water interaction remain an open issue. If a sufficiently long hydrophobic band appears in the environment, the question of its influence upon the solvent touches upon the central aspect of the mechanism which guides protein folding (as well as misfolding). It is also useful to consider the reaction of water to the presence of various types of protein surfaces.

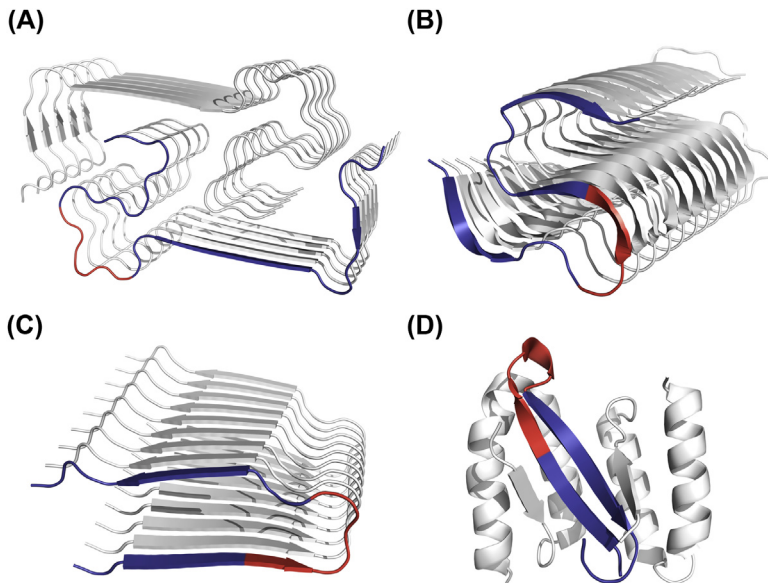


**Fig. 10.C.3** 3D presentation of location of 22–28 fragment in selected A $\beta$  fragments. (A) A $\beta$ (1–40) (2MVX). (B) A $\beta$ (11–42) (2MXU). (C) A $\beta$ (15–40) (2MPZ – protofibril). (D) A $\beta$ (16–40) (2OTK). In 2MVX, 2MXU and 2MPZ, an example chain in the fibril is shown in blue, with 22–28 fragment highlighted in red. In 2OTK, the A $\beta$ (16–40) is presented in complex with two external chains which act as its permanent chaperones.

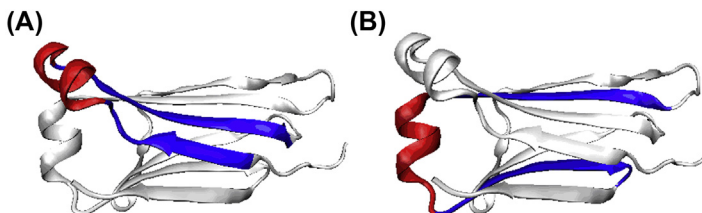


**Fig. 10.C.4** 3D presentation of C domain of light chain of IgG (7FAB, chain L). (A) location of  $\beta$ -hairpin motif (red, residues 118–124) in the 110–136 fragment (blue). (B) two  $\beta$ -strands (sand, residues 168–193) linked by helical turn (red, 178–184).

**Alternative structures solve the problem of minimization of the hydrophobic area on the surface generating the ribbon-like structural forms**

The goal of the analysis presented in this chapter is to reveal the potential structural variability of the A $\beta$ (1–40) sequence. It turns out that – much like the previously discussed cases, i.e. A $\beta$ (15–40) [7], and the tau

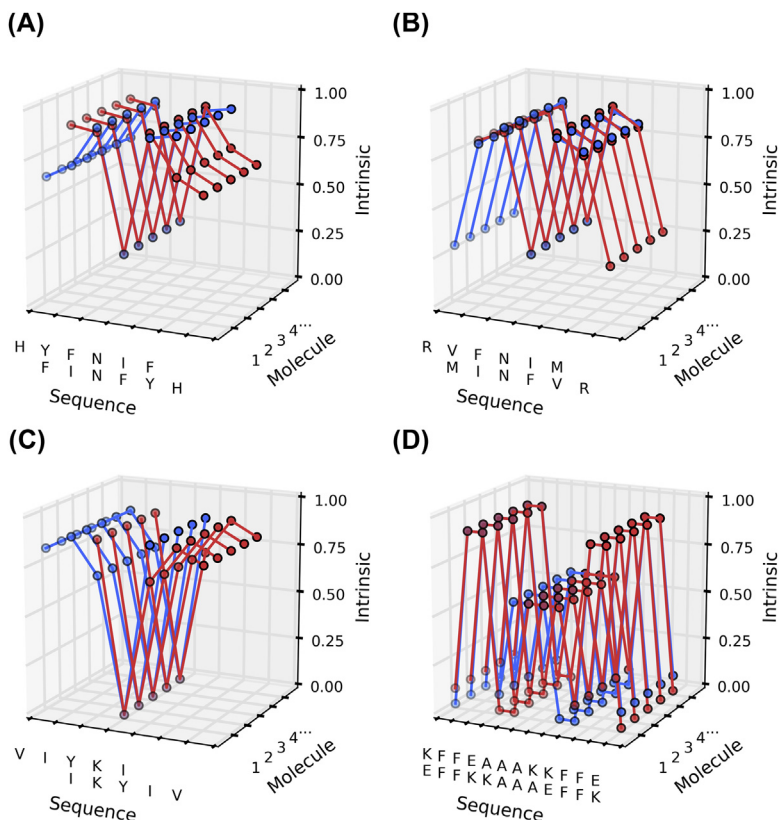


**Fig. 10.C.5** Intrinsic hydrophobicity profiles for the anti-parallel orientation of  $\beta$ -strands in peptides described in Ref. [5]: blue — top sequence, red — bottom sequence. (A) HYFNIF; (B) RVFNIM; (C) VIYKI, (D) KFFEAAAKKFFE.

amyloid [8] — such chains are possibly able of producing globular structures. This observation is supported by results of simulations carried out using specialized folding software (I-Tasser and Robetta) (Chapter 10.B).

The capability to produce a monocentric hydrophobic core suggest that such structures may emerge under real-world conditions, even in the absence of a guiding factor (i.e. in the case of Robetta models). Consequently, we may speculate that the specific structural pattern adopted by a polypeptide chain depends on its environment and that in some cases environmental conditions may favor creation of structures dominated by intrinsic hydrophobicity.

In [9] the authors postulate that even minute structural changes in the solvent may shift the balance toward oligomerization and fibrillarization.

This suggestion is quantitatively supported by simulations carried out using the fuzzy oil drop model, where deviations from the theoretical distribution of hydrophobicity — both local and global — may result in formation of elongated fibrillar forms. The comparison of globular molecules versus the amyloid is shown also in Chapter 9.

Given our objective — i.e. devising a way to identify amyloid seeds — modifying the 22–28 fragment of A $\beta$  in order to produce a helical fold is a useful test of the presented theory.

## References

- [1] Sgourakis NG, Yau W-M, Qiang W. Modeling an in-register, parallel “Iowa” A $\beta$  fibril structure using solid-state NMR data from labeled samples with rosetta. *Structure* 2015; 23(1):216–27. <https://doi.org/10.1016/j.str.2014.10.022>.
- [2] Hoyer W, Grönwall C, Jonsson A, Ståhl S, Hård T. Stabilization of a  $\beta$ -hairpin in monomeric Alzheimer’s amyloid- $\beta$  peptide inhibits amyloid formation. *Proceedings of the National Academy of Sciences* 2008;105(13):5099–104. <https://doi.org/10.1073/pnas.0711731105>.
- [3] Saul FA, Poljak RJ. Crystal structure of human immunoglobulin fragment Fab new refined at 2.0 Å resolution. *Proteins: Structure, Function, and Genetics* 1992;14(3): 363–71. <https://doi.org/10.1002/prot.340140305>.
- [4] Ghoulane A, Joseph AP, Bornot A, de Brevern AG. Analysis of protein chameleon sequence characteristics. *Bioinformatics* 2009;3(9):367–9. PMID:PMC2732029.
- [5] Al-Garawi ZS, Morris KL, Marshall KE, Eichler J, Serpell LC. The diversity and utility of amyloid fibrils formed by short amyloidogenic peptides. *Interface Focus* 2017;7(6): 20170027. <https://doi.org/10.1098/rsfs.2017.0027>.
- [6] Marshall KE, Vadukul DM, Dahal L, Theisen A, Fowler MW, Al-Hilaly Y, Serpell LC. A critical role for the self-assembly of Amyloid- $\beta$ 1–42 in neurodegeneration. *Scientific Reports* 2016;6(1). <https://doi.org/10.1038/srep30182>.
- [7] Dułak D, Banach M, Gadzała M, Konieczny L, Roterman I. Structural analysis of the A $\beta$ (15–40) amyloid fibril based on hydrophobicity distribution. *Acta Biochimica Polonica* 2018. [https://doi.org/10.18388/abp.2018\\_2647](https://doi.org/10.18388/abp.2018_2647).
- [8] Dułak D, Gadzała M, Banach M, Ptak M, Wiśniowski Z, Konieczny L, Roterman I. Filamentous aggregates of tau proteins fulfil standard amyloid criteria provided by the fuzzy oil drop (FOD) model. *International Journal of Molecular Sciences* 2018; 19(10):2910. <https://doi.org/10.3390/ijms19102910>.